

Ubiquitin-specific protease 2a stabilizes MDM4 and facilitates the p53-mediated intrinsic apoptotic pathway in glioblastoma

Chun-Lin Wang^{1,2,†}, Jun-Yu Wang^{1,†}, Zhen-Yang Liu^{1,†},
Xiao-Mei Ma³, Xiao-Wen Wang¹, Hai Jin¹,
Xiao-Ping Zhang^{4,5}, Da Fu⁴, Li-Jun Hou¹ and
Yi-Cheng Lu^{1,*}

¹Department of Neurosurgery, Shanghai Changzheng Hospital, Second Military Medical University, Shanghai 200003, China, ²Department of Neurosurgery, the 105th Hospital of PLA, Hefei 230000, Anhui Province, China, ³Department of Pathology, Shanghai Changzheng Hospital, Second Military Medical University, Shanghai 200003, China, ⁴The Key Laboratory of Stem Cell Biology, Institute of Health Sciences, Shanghai Institutes for Biological Sciences, Chinese Academy of Sciences/Shanghai JiaoTong University School of Medicine, 225 South Chongqing Road, Shanghai 200025, China and ⁵Department of Nuclear Medicine, Shanghai 10th People's Hospital, Tongji University School of Medicine, 301 Yan Chang Road, Shanghai 200072, China

*To whom correspondence should be addressed. Tel: +86 21 81885675;
Fax: +86 21 81885675;
Email: luyicheng1947@163.com

Correspondence may also be addressed to Li-Jun Hou.
Tel: +86 21 81886811; Fax: +86 21 81885675;
Email: lijunhou2010@163.com

The mouse double minute 4 (MDM4) oncoprotein may inhibit tumorigenesis by regulating the apoptotic mediator p53. Ubiquitin-specific protease 2a (USP2a) is a deubiquitinating enzyme that protects MDM4 against degradation, so USP2–MDM4 interaction may be a key determinant of the malignant potential of human cancers. MDM4 and USP2a, as well as the MDM4–USP2a complex, were more highly expressed in glioblastoma multiforme tissue samples from patients with good prognosis compared with patients with poor prognosis. Analysis of the prognostic parameters indicated that MDM4 expression was positively correlated with an increased likelihood for survival. Compared with the poor prognosis patients, mitochondria from good prognosis glioma patients contained higher levels of both MDM4 and the proapoptotic protein p53Ser46^P. In U87MG glioma cell line, the overexpression of MDM4 enhanced ultraviolet (UV)-induced cytochrome c release and apoptosis. In contrast, MDM4 knockdown decreased mitochondrial p53Ser46^P levels and rescued cells from UV-induced apoptosis. The expression of MDM4 and USP2a were positively correlated with each other. MDM4–USP2a complexes were found only in the cytoplasmic fraction, whereas the mitochondrial fraction contained MDM4–p53Ser46^P and MDM4–Bcl-2 complexes. Overexpression of USP2a increased p53 and p53Ser46^P levels in the mitochondria, whereas simultaneous MDM4 knockdown completely reversed this effect. UV-induced apoptosis was reduced by USP2a knockdown but restored by the simultaneous overexpression of MDM4. This apoptotic response was reduced by knockdown of p53 but not p21. Our results suggest that USP2a binds to and stabilizes MDM4; thus in turn, it enhances the mitochondrial localization of p53 and promotes apoptosis in glioma cells.

Introduction

Gliomas are brain tumors that originate from glial cells in the brain or spinal cord (1,2) and are the most common primary tumors of the

Abbreviations: BCNU, 1,3-bis(2-chloroethyl)-1-nitrosourea; MDM4, mouse double minute 4; PBS, phosphate-buffered saline; shRNA, short hairpin RNA; USP, ubiquitin-specific protease; UV, ultraviolet.

[†]These authors contributed equally to this work.

central nervous system. Glioblastoma multiforme is the most aggressive form of glioma and has the lowest 2-year survival rate due to a strong apoptotic resistance in the individual tumor cells (3). Similar to other forms of cancer, the reduced expression of tumor suppressors and proapoptotic proteins has been implicated in the development of gliomas.

Mouse double minute 4 (MDM4), formerly MDMX, is a member of the mouse double minute oncoprotein family, which includes the full-length MDM2, MDM4 and their derivate minor forms. Both full-length MDM4 and MDM2 demonstrated oncogenic potential via inhibition of tumor suppressor p53 (4,5). However, MDM4 may also play an inhibitory role in tumorigenesis under certain conditions. The rate of tumor formation in MDM2 transgenic mice was accelerated when MDM4 was simultaneously deleted (6). Furthermore, both overexpressed and endogenous MDM4 stabilized active p53 by counteracting MDM2-mediated degradation (7–9), and MDM4 overexpression promoted p53-mediated apoptosis under stress conditions (10). A recent report demonstrated that MDM4 facilitated the p53-mediated intrinsic apoptotic pathway by acting as a p53Ser46^P docking site to facilitate the binding of p53Ser46^P to antiapoptotic Bcl2 (11). Previous studies also demonstrated the amplification and overexpression of MDM4 in malignant gliomas without p53 mutation or MDM2 overexpression (12,13). However, the oncogenic and antitumor functions of MDM4 in gliomas in different genetic backgrounds remain unclear.

The transcription factor p53 is implicated in cell cycle arrest, DNA repair, senescence and apoptosis (14,15). The inactivation of p53 is a critical step in tumorigenesis (15), and mutation or deletion of p53 has been found in nearly half of all human cancers (16). The p53 protein activates apoptosis through two distinct pathways: through the transcriptional activation of proapoptotic genes and through facilitation of the mitochondrial outer membrane permeabilization pathway, which results in the release of the apoptotic trigger, cytochrome c, into the cytosol (17). The mitochondrial localization of p53 is a prerequisite for the regulation of mitochondrial outer membrane permeabilization (18,19).

The ubiquitin-specific proteases (USPs) are a group of cysteine proteases within the general class of deubiquitinating enzymes (20,21). USP 2a (USP2a) is a deubiquitinating enzyme that can deubiquitinate MDM2, an E3 ubiquitin ligase, without reversing the MDM2-mediated ubiquitination of p53. Upregulation of USP2a promoted MDM2 accumulation, MDM2-mediated ubiquitination and p53 degradation (22). This antiapoptotic action may explain the canonical oncogenic properties of USP2a in prostate cancer (23). However, MDM4 is also a substrate of USP2a. Indeed, USP2a can deubiquitinate MDM4 and prevent its degradation by MDM2 (24), suggesting that USP2a may promote or suppress p53-dependent apoptosis depending on the balance between MDM2 and MDM4 expression.

We analyzed the expression of USP2a and MDM4 in human glioblastoma multiforme. USP2a and MDM4 were more highly expressed in tumor samples from patients with good prognosis, and good prognosis tissue exhibited increased release of cytochrome c from the mitochondria. The overexpression of USP2a stabilized MDM4 by complex formation and facilitated the p53-dependent, but p21-independent, intrinsic apoptotic pathway in U87MG glioma cell line. These results suggest that MDM4 is a potential therapeutic target in glioma.

Materials and methods

Cell culture, plasmid construction, transfection and ultraviolet irradiation

U87MG human glioma cell line was obtained from the American Type Culture Collection. Cells were cultured in Dulbecco's Modified Eagle's Medium supplemented with 10% fetal calf serum (Life Technologies, Gaithersburg, MD), penicillin G (100U/ml) and streptomycin (100mg/ml) at 37°C in a

5% CO₂ atmosphere. Transfections were performed using Lipofectamine 2000 (Invitrogen, Carlsbad, CA). The full-length complementary DNAs of the human p53, human MDM4, human MDM2 and human p21 genes were isolated from HEK293T cells using reverse transcription–polymerase chain reaction. Human USP2a complementary DNA was isolated from LNCaP cells using reverse transcription–polymerase chain reaction. All PCR products were ligated into pcDNA3, p53 was also cloned into pEGFP-C1 (Clontech, Mountain View, CA), and MDM4 was also cloned into p3XFlag-CMV-10 (Sigma–Aldrich, St Louis, MO). Human Myc-USP2a was cloned by PCR using primers that incorporated the myc epitope at the 5' end. U87MG cells were infected with short hairpin RNA (shRNA) lentivirus with green fluorescent protein expression, and after sorting, cells were transfected with plasmid. At 24 h posttransfection, U87MG cells were kept under a lethal amount of ultraviolet (UV)-C irradiation (40 J/m²) for 8 h and then harvested.

Tumor samples

The tumor samples were selected from the tumor tissue from primary glioma patients that is preserved in the Cancer Tissue Bank at Changzheng Hospital in Shanghai, China. Informed consent for the experimental use of the surgical samples was obtained from all patients. All specimens were sampled from tumors at the time of surgery, snap frozen in liquid nitrogen and stored at –80°C until retrieved for experiments. Clinical specimens were divided into two groups: a good prognosis group (from patients with survival time ≥12 months) and a poor prognosis group (with survival time <12 months).

Isolation of mitochondrial, cytoplasmic and total protein lysates

To obtain total cellular protein lysates, cultured cells or tissues were harvested, washed twice in ice-cold phosphate-buffered saline (PBS) and lysed in RIPAII [500 mM NaCl, 50 mM Tris (pH 7.4), 0.1% sodium dodecyl sulfate, 1% NP-40, 0.5% Na-DOC, 0.05% Na₂S₂O₈ and complete protease inhibitor mix] for 30 min on ice. Lysates were sonicated and centrifuged at 12 000g. The supernatants were used as the total cell lysates. For isolating the mitochondria, the cells or tissues were washed twice in ice-cold washing buffer [10 mM Tris (pH 7.5) and 200 mM sucrose] and resuspended in methylene blue buffer [250 mM sucrose, 20 mM Tris (pH 7.5), 10 mM KCl, 1.5 mM MgCl₂, 1 mM ethylenediaminetetraacetic acid, 1 mM ethyleneglycol-bis(aminoethyl ether)-tetraacetic acid, 1 mM dithiothreitol and complete protease inhibitor cocktail]. After hypotonic swelling on ice, the cells were disrupted by passing six times through a 26-gauge needle, and the tissues were disrupted by homogenation. The suspension was then centrifuged at 750g at 4°C. The supernatants were collected and further centrifuged at 13 000g for 10 min at 4°C. The supernatant contained the cytoplasmic fraction. The mitochondria from the pellet were lysed in RIPAII buffer to obtain the mitochondrial fraction.

Immunohistochemistry

Paraformaldehyde-fixed (4%) and paraffin-embedded tissues were sectioned at 3 μm. The expression levels and subcellular distributions of MDM4, p53, USP2a, MDM2 and activated (cleaved) caspase 3 in glioma tissue sections were detected using primary antibodies (listed below), biotinylated secondary antibodies and the ABC reagent (Vector Labs, Burlingame, CA) with 3,3'-diaminobenzidine hydrochloride (Sigma) as the substrate. Expression levels were measured using the number of cells with detectable immunoreactivity (high expression: higher than the average percentage of positive cells; low expression: lower than the average proportion of positive cells) by an observer blind to the prognosis.

Immunofluorescence in glioma cell lines

After various experimental treatments, the adherent cultured cells were washed twice with cold PBS and fixed in a paraformaldehyde solution (4% in PBS, pH 7.4) for 30 min at 4°C. The fixed cultures were then washed twice with PBS, treated with permeabilization solution (0.1% Triton X-100 in 0.1% sodium citrate) on ice for 2 min and incubated in blocking buffer (3% bovine serum albumin in Tris-buffered saline with Tween 20) for 1 h. The cells were then incubated with the indicated antibody in Tris-buffered saline with Tween 20 containing 3% bovine serum albumin overnight at 4°C. After the incubation, the cells were washed and incubated with the indicated fluorescence-labeled secondary antibody in the dark at 37°C for 1 h. After washing, the cells were observed under a fluorescence microscope. Confocal images were captured using a Leica TCS SP5 confocal microscope.

Immunoprecipitation and immunoblotting

A sample of the indicated lysate containing 1 mg of total protein was precleared with protein A-Sepharose for 1 h at 4°C and immunoprecipitated with 2 μg of the indicated primary antibody using gentle rocking at 4°C overnight. Protein A-Sepharose was then added, and the mixture was incubated for an additional 1 h at 4°C. The beads were recovered and washed three times with the lysis buffer to elute the proteins. Proteins were separated by sodium dodecyl sulfate–polyacrylamide gel electrophoresis, transferred onto polyvinylidene

difluoride membranes (Millipore) and visualized using enhanced chemiluminescence (ECL Amersham).

Antibodies

The anti-MDM4 (M0445), anti-MDM2 (SAB4501849), anti-α-tubulin (T8203) and anti-Flag (F7425) antibodies were got from Sigma–Aldrich. The anti-Bcl2 (sc-130308), anti-p53 (sc-56181), anti-BCL2 (sc-7382), anti-cytochrome c antibody (sc-13156) and anti-p21 antibody (sc-756) were got from Santa Cruz. The anti-c-myc antibody (9E10) was got from Pharmingen. The anti-p53Ser46^P (2521), anti-p53Ser15^P (9284), anti-caspase 3 (cleaved, 9664) and anti-glyceraldehyde 3-phosphate dehydrogenase (2118) antibodies were got from Cell Signaling. The anti-CoxIV antibody (A21348) was got from Molecular Probes–Invitrogen, the anti-USP2a antibody (AB501) was from Lifesensors and the anti-rabbit IgG antibody (31239) was from Pierce.

The following second antibodies were used: Cy5-labeled goat anti-rabbit IgG (PA45004, GE Healthcare Chalfont, St Giles, UK), Alexa Fluor 488-labeled anti-p53Ser46^P and Alexa Fluor 546 goat anti-mouse IgG (A-11003, Molecular Probes), horseradish peroxidase-labeled goat anti-mouse IgG (sc-2005, Santa Cruz) and horseradish peroxidase-labeled goat anti-rabbit IgG (sc-2004, Santa Cruz).

RNA interference

To construct specifically targeted shRNA expression plasmids, two complementary DNA oligonucleotides containing the target sequence were synthesized, annealed and inserted between the BbsI and XhoI restriction sites of the pBS-hU6-I plasmid. The fragment containing the human U6-RNA Pol III promoter and the shRNA were subcloned into FG12 between the XbaI and XhoI sites. The target sequences were GTCCTGATTGTCGAAGAA (MDM4, AF007111), GGTTACTGTTCTACGGTCT (USP2a, NM_004205), GTAATCTACTGGGACGGAA (p53, NM_000546.4), GAAGTTGAATCTCTCGACT (MDM2, NM_002392.3) and GCATGACAGATTTCTACCA (p21, NM_078467.2). Recombinant lentiviruses were produced by transiently transfecting HEK293T cells with the lentiviral packaging constructs pMDLg/pRRE and pRSV/REV, the vesicular stomatitis virus glycoprotein-expressing plasmid pHCMVG and the shRNA expression vector using the calcium phosphate method as described previously (25). U87MG cells were transduced with concentrated lentivirus stocks at the same multiplicity of infection in the presence of 4 μg/ml of polybrene. Protein was harvested from the infected cells after 72 h and used for immunoblotting to measure knockdown efficiency.

Viability and apoptosis detection

The cell proliferation was assessed using 3-(4,5-dimethylthiazole-2-yl)-2,5-diphenyl tetrazolium bromide assay. Briefly, cells were seeded into 96-well plates (1 × 10⁴ cells/well) and grown for 1, 2, 3, 4 or 5 days. Then, 20 μl of 3-(4,5-dimethylthiazole-2-yl)-2,5-diphenyl tetrazolium bromide (0.5 mg/ml) was added along with 200 μl of medium into each well. The cells were then incubated for 3 h at 37°C, and the converted dye (formazan) was solubilized with acidic isopropanol (0.04–0.1 μM HCl in absolute isopropanol). The absorbance of the converted dye was measured at 590 nm. Apoptosis was monitored by annexin V binding using annexin V assay (Clontech) according to the manufacturer's instructions.

Real-time PCR

Total RNA was extracted from cells using TRIzol reagent (Invitrogen) and reverse transcribed using M-MLV Reverse Transcriptase (Promega). Real-time PCR was performed using an ABI 7500 fast sequence detection system (Applied Biosystems) with a SYBR green fluorescent label. Reaction mixtures (10 μl final volume) contained 1 μl of Power SYBR Green PCR Master Mix (Applied Biosystems), 3–5 pmol of each primer and 0.25 μl of the RT reaction. Samples were run in triplicate in optically clear 96-well plates (Corning, NY). The thermocycling parameters were as follows: 95°C for 10 min, followed by 40 cycles of 95°C for 15 s, 60°C for 1 min and an extension/detection step at 72°C for 30 s. Each RNA sample was run in triplicate. The primer sequences used were MDM4 (197 bp): 5'-CTCAGTGCAACATCTGACAG-3' (F) and 5'-CATATGCTGCTCCTGCTGATC-3' (R); MDM2 (224 bp): 5'-TCCAGCTTCGGAACAAGAGACCT-3' (F) and 5'-TCACGA GAAGCTTGGCACGCC-3' (R); USP2a (185 bp): 5'-CTATGGGG CCAATCTGGCTGCCT-3' (F) and 5'-TCTGGCTCTCTGCCGCTTACC-3' (R); p53 (111 bp): 5'-TGGTGCCTATGAGCCGCT-3' (F) and 5'-TGGTGAG GATGGCCCTCCGG-3' (R); p21 (227 bp): 5'-TGGCACAGGCC TTAGAGT-3' (F) and 5'-ATGAGCCACGTGGCATGCC-3' (R); 36B4 (157 bp): 5'-GTGACATCGTCTTTAAACCCCTCG-3' (F) and 5'-GGAT CTGCTGCATCTGCTTGGAGC-3' (R).

Statistical analyses

The relationships between MDM4 expression and the expression of USP2a, p53 or p53Ser46^P were evaluated using the chi-square test. Univariate survival analysis was performed using the Kaplan–Meier method and analyzed using

the log-rank test to assess the survival differences between the groups. The Cox proportional hazards model for multivariate survival analysis was used to assess predictors related to survival. A two-tailed *P*-value of <0.05 was considered to be statistically significant. Analyses were performed using the SPSS 10.0 statistical software for Windows (SPSS).

Results

Higher MDM4 and USP2a protein levels in good prognosis gliomas are accompanied by enhanced apoptosis

Two groups of high-grade glioma samples were collected, one group from patients with good prognosis as defined by patients surviving 12 months or longer and the other group from patients with poor prognosis (<12 months). We found that good prognosis gliomas exhibited greater immunoreactivity for USP2a, MDM4, p53Ser46^P and caspase 3 proteins than poor prognosis gliomas (blue staining, **Figure 1a**), whereas MDM2 and p53 immunoreactivity did not appear to differ between the groups (**Figure 1a**). The elevated p53Ser46^P and caspase 3 in good prognosis gliomas indicated the increase of apoptosis compared with poor prognosis gliomas. Statistical analysis further determined that MDM4 expression correlated positively with USP2a and p53Ser46^P expression but not with p53 expression (**Table I**). In contrast to the immunohistochemical results, the messenger RNA levels of MDM4, p53, MDM2, USP2a and p21 were not significantly different between the two glioma outcome groups (**Figure 1b**). Immunoblotting revealed that the protein levels of USP2a, MDM4, p53Ser46^P and caspase 3 were higher in good prognosis gliomas compared with poor prognosis gliomas; however, MDM2, p53 and p21 levels were not significantly different (**Figure 1c**), which is consistent with the immunohistochemical results.

Univariate survival analysis revealed significant relationships between age at diagnosis, expression of MDM4, expression of USP2a and prognosis (**Supplementary Table S1**, available at *Carcinogenesis* Online). There was no significant association identified between prognosis and gender, tumor size, specific chemotherapy or radiotherapy. Survival probability increased in patients with USP2a- or MDM4-positive glioblastoma tissues (**Figure 1d**). Multivariate analysis using the Cox proportional hazards model for all variables included in the univariate analysis revealed that the expression of MDM4 and age at diagnosis were independent prognostic factors for patients with glioma. However, USP2a expression exhibited no significant relationship with any of these prognostic parameters in multivariate survival analysis (**Supplementary Table S1**, available at *Carcinogenesis* Online). These analyses suggest that MDM4 expression may be a key prognostic index for glioblastoma patient survival.

Greater interaction between MDM4/USP2a and MDM4/p53 in good outcome gliomas

In agreement with a previous study (24), USP2a specifically coimmunoprecipitated with MDM4 (**Figure 2a**) and more MDM4–USP2a complex was identified in good versus poor prognosis gliomas. The total amount of the MDM4–USP2a complex increased upon higher expression of the individual MDM4 and USP2a proteins. It has been reported that mitochondrial MDM4 facilitates the mitochondrial localization of the proapoptotic protein p53Ser46^P (p53 phosphorylated at Ser46) (26), suggesting the possible protein–protein interaction. Indeed, immunoprecipitation revealed greatly enhanced binding of p53Ser46^P to MDM4 in the mitochondrial extract from good prognosis gliomas (**Figure 2b**). These results suggest that the p53-mediated intrinsic apoptotic pathway might reduce tumor aggression or confer greater sensitivity to chemotherapy agents.

The MDM4, p53 and p53Ser46^P protein levels were significantly higher in the mitochondrial lysates from the good prognosis patients, whereas the level of cytochrome c in the mitochondrial fraction was lower in the good prognosis glioma samples (**Figure 2d**), suggesting the enhanced release of cytochrome c into the cytosol in the good prognosis gliomas. Indeed, similar analysis of cytoplasmic fractions revealed that cytochrome c and MDM4 were elevated in the cytosolic

lysate from good prognosis glioma samples, whereas no difference was observed in the p53 or p53Ser46^P levels between the cytosolic lysates from the two glioma types (**Figure 2c**).

MDM4 promoted U87MG cell apoptosis through a p53-dependent mitochondrial pathway after UV irradiation

The expression of MDM4 was correlated with elevated cytosolic cytochrome c, suggesting enhanced apoptosis. In U87MG cells transfected with p53, the overexpression of MDM4 led to elevated levels of cleaved (activated) caspase 3 and the release of cytochrome c from the mitochondria compared with cells transfected with p53 alone (**Figure 3a**). In addition, MDM4 overexpression enhanced both cleaved caspase 3 formation and the release of cytochrome c induced by UV irradiation compared with cells treated only with UV. In contrast, MDM4 overexpression inhibited 1,3-bis(2-chloroethyl)-1-nitrosourea (BCNU)-induced cell apoptosis (**Supplementary Figure S1**, available at *Carcinogenesis* Online), suggesting that UV irradiation and BCNU treatment might induce different signaling pathways related to apoptosis in U87MG cells. On the other hand, both cleaved caspase 3 expression and mitochondrial cytochrome c expression were significantly lower in U87MG cells cotransfected with p53 and the shRNA-targeting MDM4 (**Figure 3a**). Thus, MDM4 expression was positively correlated with the activation of caspase 3.

Mitochondrial MDM4 was reported to facilitate both the localization of the proapoptotic p53Ser46^P protein to the mitochondria and the p53-mediated release of cytochrome c (11). To identify whether MDM4 also has these effects on glioma cells, we deplete MDM4 efficiently by making use of the MDM4 shRNA (**Figure 3b**). Compared with the non-transfected UV-treated cells, in U87MG cells transfected with MDM4 shRNA, the expression levels of p53 and p53Ser46^P were significantly lower in both the cytoplasmic and mitochondrial protein extracts following UV irradiation. Consistent with the reduced apoptosis observed in the UV-treated MDM4 shRNA-transfected cells, cytochrome c in the cytoplasmic extract of UV-treated MDM4 shRNA-transfected cells was significantly lower compared with the UV-treated non-transfected cells (**Figure 3c**). The reduced UV-induced apoptosis in MDM4 shRNA-transfected glioma cells was confirmed using a direct apoptotic assay (**Figure 3d**). This assay demonstrated lower annexin V staining in cells transfected with MDM4 shRNA (reduced MDM4 expression). The apoptosis was enhanced by the overexpression of MDM4 in U87MG cells, whereas MDM4 knockdown reduced apoptosis. These results were then confirmed by the direct quantitation of apoptotic cells (**Figure 3e**).

We next studied the effects of p53 on MDM4-induced cell apoptosis (**Figure 3f**). Enhanced apoptosis induced by MDM4 overexpression was abrogated by transfection with p53 shRNA, indicating that MDM4 promoted p53-dependent apoptosis. In addition, we found that USP2a increased the mitochondrial enrichment of transcriptionally inactive p53, and either MDM4 or USP2a could promote cell death in cisplatin-treated U251 cells expressed with mutant p53 (R273H) that lacks transcriptional activity (**Supplementary Figure S2**, available at *Carcinogenesis* Online), indicating that MDM4 and USP2a regulated p53-mediated cell apoptosis not through inhibiting p53 transcriptional activity.

MDM4 interacts with p53Ser46P, USP2a and Bcl2 in UV-treated U87MG cells

One previous study (24) demonstrated that USP2a can stabilize MDM4 protein by preventing MDM2-dependent degradation. Similar to the glioma tissue samples (**Figure 2**), we found that endogenous MDM4 coimmunoprecipitated with USP2a from U87MG whole-cell extracts (**Figure 4a**); however, no USP2a–MDM4 complex formation was detected by immunoprecipitation using the mitochondrial extract (**Figure 4b**). We also detected interaction between MDM4 and p53Ser46^P and between MDM4 and Bcl2 in the mitochondrial extract from the UV-treated U87MG cells (**Figure 4c and d**). Similar to what we observed with p53Ser46^P, more Bcl2 interacted with MDM4 in the mitochondrial extract after UV treatment (**Figure 4d**). Furthermore,

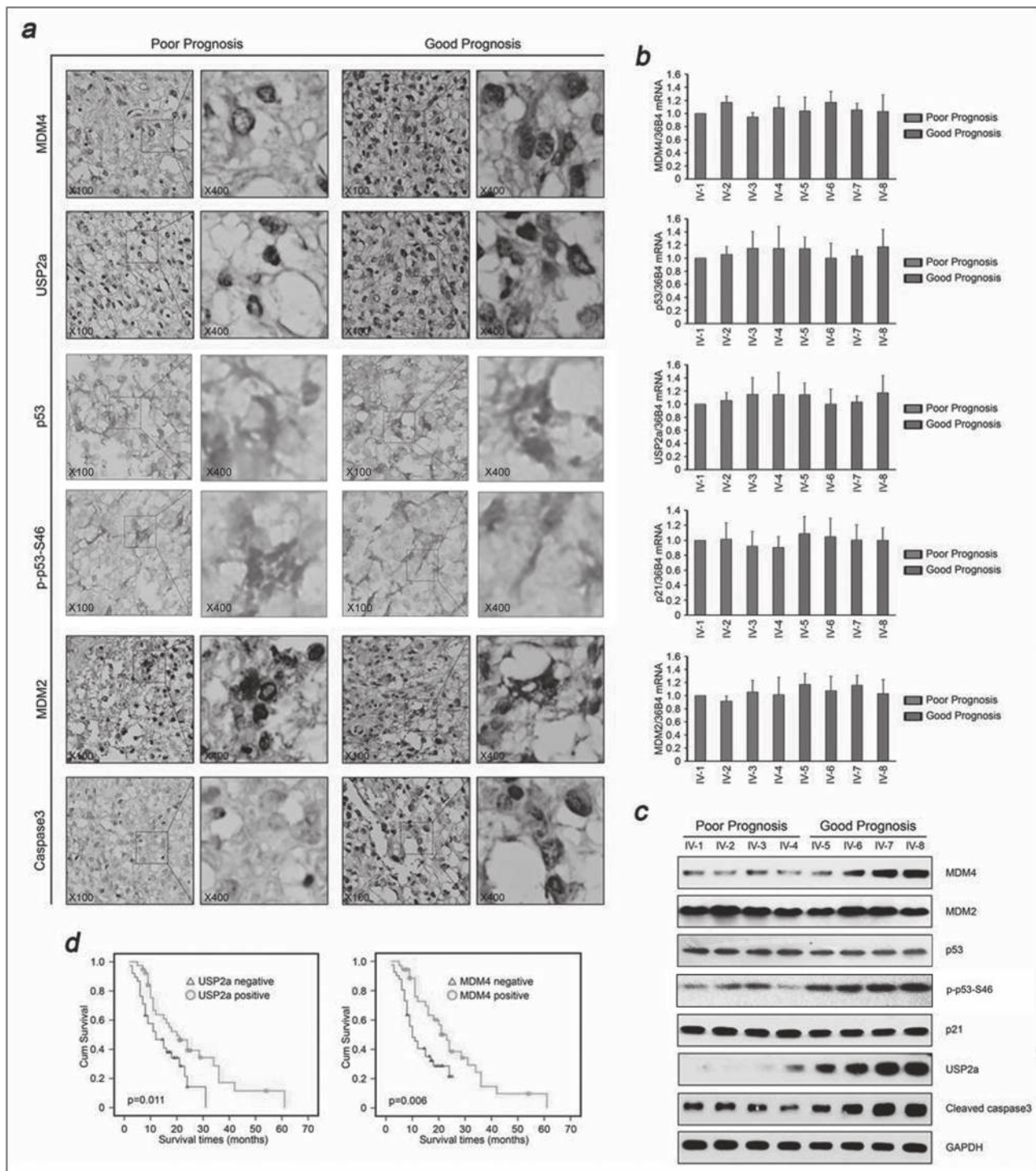


Fig. 1. The expression of USP2a, MDM4, MDM2, p53, p53Ser46^P, caspase 3 and p21 in gliomas. (a) USP2a, MDM4, MDM2, p53, p53Ser46^P and caspase3 were detected in IV grade gliomas by immunohistochemistry. Tissue samples were from either poor prognosis or good prognosis glioma patients. (b) The messenger RNA levels of USP2a, MDM4, MDM2, p53 and p21 were measured in gliomas by real-time PCR. Tissue samples 1–4 were from poor prognosis gliomas, whereas samples 5–8 were from good prognosis gliomas. The 36B4 transcript was used in each sample as an internal reference standard to control for variations in the messenger RNA content and quantity. (c) The protein levels of USP2a, MDM4, MDM2, p53, p53Ser46^P, caspase 3 and p21 in gliomas. Tissue samples 1–4 were from poor prognosis gliomas, whereas samples 5–8 were from good prognosis gliomas. Glyceraldehyde 3-phosphate dehydrogenase was used as the internal control. (d) Kaplan–Meier curves of survival durations in patients with glioblastomas according to USP2a and MDM4 expression.

we examined the subcellular location of p53, p53Ser46^P, MDM4 and USP2a using immunofluorescence staining (Figure 4e). Confocal imaging revealed that MDM4 only partially colocalized with p53, but MDM4 was highly colocalized with p53Ser46^P and USP2a (Figure 4e), consistent with the results of the immunoprecipitation and immunoblotting analyses.

When stabilized by USP2a, MDM4 promoted p53-mediated intrinsic apoptosis in UV-treated U87MG cells

To further study the relationship between USP2a, MDM4 and p53 in UV-induced apoptosis of U87MG cells, we introduced knockdown of USP2a and p21, as well as relevant p53 and MDM2. The knockdown

Table I. Relationship between MDM4 expression and USP2a, p53 or p53Ser46^P expression in tumor specimens from 77 patients with good or poor prognosis glioblastoma

	Protein expression	USP2a		<i>P</i>	P53		<i>P</i>	p-p53Ser46		<i>P</i>
		High	Low		High	Low		High	Low	
		MDM4	High	28	8	0.01	11	25	0.577	27
	Low	11	30		15	26		17	24	

Pearson chi-square test.

efficiency of each gene was confirmed by immunoblotting (Figure 5a–d). As indicated in Figure 5e and Supplementary Figure S3a, available at *Carcinogenesis* Online, we found that overexpression of USP2a in U87MG cells led to increase of MDM4 protein levels but not p53 or MDM2. When silencing the expression of USP2a using a specifically targeted shRNA, the expression of MDM4 protein decreased, whereas the p53 expression level remained unchanged (Figure 5e). These results indicate that USP2a stabilized MDM4 in U87MG cells but did not affect the whole-cell expression of p53.

Because MDM4 associated with p53 in the mitochondria (Figure 4c–e), we investigated whether USP2a could enhance mitochondrial p53 expression and phosphorylation at Ser46 by stabilizing MDM4. As shown in Figure 5f, overexpression of USP2a increased p53 and p53Ser46^P levels in the mitochondrial extract, whereas overexpression of p21 had no such effect. Simultaneous overexpression of USP2a and shRNA-mediated knockdown of p21 still increased p53 and p53Ser46^P levels in the mitochondrial extract, whereas the knockdown of MDM4 completely abrogated the increase in the levels of mitochondrial p53 and p53Ser46^P in cells overexpressing USP2a (Figure 5f and Supplementary Figure S3b, available at *Carcinogenesis* Online). These results revealed that MDM4, but not p21, was necessary for the increase in mitochondrial p53 and p53Ser46^P levels in USP2a-overexpressing U87MG cells, thus indicating that MDM4 mediates the subcellular translocation of p53 and p53Ser46^P to the mitochondria in cells overexpressing USP2a.

Apoptosis in U87MG cells was reduced by USP2a shRNA but restored by the simultaneous overexpression of MDM4 (Figure 5g and Supplementary Figure S3c, available at *Carcinogenesis* Online). This again suggests that USP2a promoted U87MG cell apoptosis by stabilizing MDM4. We also investigated the effects of MDM2 and p21 on MDM4-mediated U87MG cell apoptosis following UV irradiation. As shown in Figure 5h and Supplementary Figure S3d, available at *Carcinogenesis* Online, neither knockdown of p21 nor MDM2 could affect MDM4-mediated U87MG cell apoptosis, as reflected by the lack of either cleaved caspase 3 or released cytochrome c.

The apoptosis assay indicated that UV-induced apoptosis in U87MG cells was inhibited by USP2a knockdown but not by p21 knockdown (Figure 5i and j). In addition, we also observed no difference in the expression of p21 downstream target genes including PUMA, Noxa and Perp between the control as well as MDM4 overexpression and knockdown groups after UV treatment (Supplementary Figure S4, available at *Carcinogenesis* Online). Overall, these data indicated that USP2a was involved UV-induced U87MG cell apoptosis likely by stabilizing MDM4, which in turn potentiated the p53-mediated apoptosis pathway in the mitochondria (but was not a p53–p21 pathway).

Discussion

Malignant gliomas are the most common primary tumors of the central nervous system and are often resistant to treatment. By analyzing protein expression, subcellular localization and protein–protein interaction, we found that USP2a, MDM4 and the USP2a–MDM4 complex were highly expressed in high-grade gliomas with good prognosis. By analyzing the relationship between USP2a and MDM4 expression in the U87MG and U251 glioma cell lines, we present strong evidence that USP2a stabilizes mitochondrial MDM4, which in turn acts as an

anchor for p53Ser46^P, thereby facilitating the p53-dependent intrinsic apoptotic pathway.

Both MDM4 and MDM2 were shown to be crucial inhibitors of the tumor suppressor p53 protein (4,5), and MDM4 is considered to be a negative regulator of the growth arrest mediated by p53 (27). In a previous report, Jin *et al.* (28) described that the inducible overexpression of MDM4 promotes proliferation and the chemotherapeutic agent BCNU resistance in a glioblastoma cell line. The result in Supplementary Figure S1, available at *Carcinogenesis* Online, was in agreement with this previous report. UV irradiation and BCNU treatment might induce different signaling pathways, thereby causing different phenotypes in the U87MG cells. It appeared that MDM4 facilitating p53-mediated mitochondrial apoptosis might be dominant when using a lethal dose UV irradiation in U87MG cells.

USP2a was found to protect human prostate cancer from apoptosis (23) likely by facilitating MDM2 accumulation and leading to decreased p53 levels (22). Similar to MDM4, however, USP2a exhibits a markedly more complex function that is contradictory with its having a purely oncogenic action. Our results indicated that USP2a can stabilize MDM4 resulting in higher MDM4 protein levels, which in turn promote intrinsic apoptosis in glioma cells (Figure 5). Our findings are consistent with previous studies demonstrating that the rate of tumor formation is accelerated in MDM2 transgenic mice that lack both MDM4 alleles compared with mice having both alleles (6).

The MDM4–USP2a complex and the MDM4–p53Ser46^P complex were more highly expressed in good prognosis glioma tissues or UV-treated glioma cells (Figures 2a and b and 4a and c). This is consistent with the observation that USP2a binding to MDM4 protects MDM4 from MDM2-initiated proteasomal degradation, thereby allowing for MDM4–p53Ser46^P complex formation and the activation of p53-dependent apoptosis (8,24).

Cytoplasmic p53 translocates to the mitochondria only in response to apoptotic stimuli (19). The analysis of mitochondrial p53 post-translational modifications revealed the presence of mitochondrial p53Ser46^P (29), which acted as a preferential binding partner for antiapoptotic Bcl2 and a more active promoter of p53-mediated intrinsic apoptosis (26). In addition, transgenic mice carrying the human mutant p53S46A displayed a significant decrease in thymocyte apoptosis (30), indicating that p53 exerts an important proapoptotic function in thymus tissue (31). Our results demonstrated that MDM4 inhibited U87MG cell proliferation and promoted p53-dependent apoptosis (Figure 3e and f).

Indeed, p53 activates apoptosis through two distinct pathways: the transcriptional activation of proapoptotic genes and the facilitation of mitochondrial outer membrane permeabilization with the release of cytochrome c (17). Mitochondrial p53 was phosphorylated at Ser46, a modification associated with proapoptotic activity. Notably, severe, irreparable DNA damage induces phosphorylation at Ser46, and Ser46 phosphorylated p53 selectively transactivates proapoptotic genes. The canonical p53–p21 pathway promoted apoptosis via the activation of downstream target genes. We further examined the expression of related genes including PUMA, Noxa and Perp (30). We observed no difference in the expression levels of these genes between the control and MDM4 overexpression and knockdown groups after UV treatment. It was reported that MDM4 does not possess intrinsic ubiquitin E3 ligase activity against p53 *in vivo* but rather binds to p53 and inhibits its transcriptional activity (32,33). Because U87MG cells

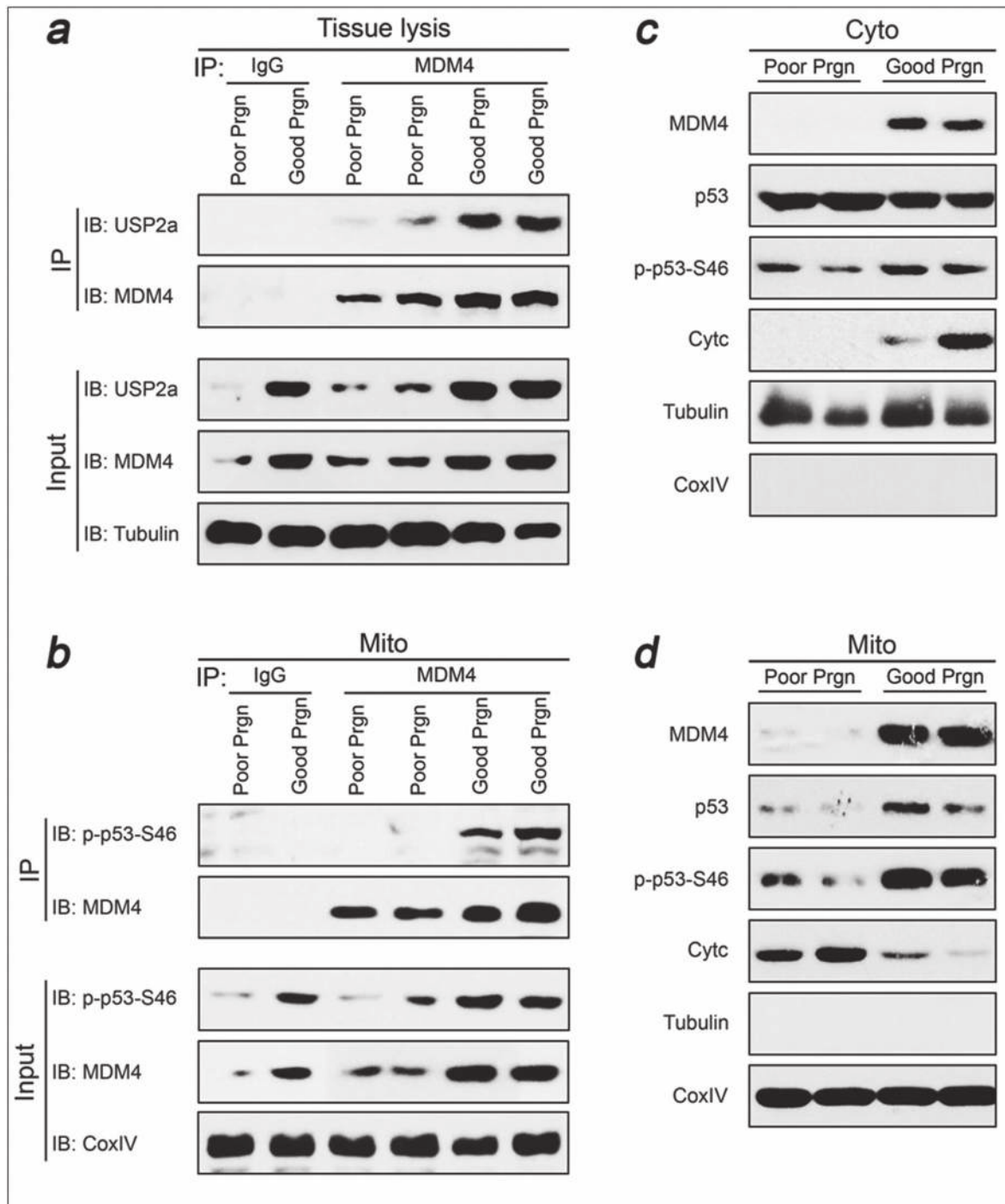


Fig. 2. MDM4 interacts with USP2a and p53Ser46^P in glioma tissues. (a) MDM4 interacted with USP2a in gliomas. Glioma lysates from good and poor prognosis patients were incubated with an anti-MDM4 antibody or an anti-IgG control and then analyzed by immunoblotting with anti-USP2a antibody and anti-MDM4 antibody. Separate aliquots of the lysates were immunoblotted with the indicated antibodies. Samples were from poor prognosis and good prognosis gliomas. (b) MDM4 interacted with p53Ser46^P in the mitochondrial extract from good prognosis gliomas. The mitochondria extract was immunoprecipitated with anti-MDM4 antibody and analyzed by immunoblotting with anti-p53Ser46^P antibody and anti-MDM4 antibody. Separate aliquots of the lysates were immunoblotted with the indicated antibodies. The purity of the mitochondrial lysate was examined by immunoblotting with anti-CoxIV antibody. Samples were from poor and good prognosis gliomas. (c, d) The subcellular distribution of MDM4, p53, p53Ser46^P, p53Ser15^P and cytochrome c in the mitochondrial and cytoplasmic fractions. The purity of the mitochondria and cytoplasmic fractions was examined by immunoblotting with anti-CoxIV and antitubulin antibodies, respectively. Samples were from poor and good prognosis gliomas.

express wild-type p53, we used a known dominant negative mutant cell line, U251. U251 expresses mutant p53 (R273H) that lacks transcriptional activity (34,35). Cisplatin is a widely used chemotherapeutic agent that is generally recognized as a DNA-damaging drug. It has been reported that the mitochondrial accumulation of

p53 and caspase-dependent mitochondrial apoptosis are specifically disrupted in ovarian cancer cells that are resistant to cisplatin treatment (36). We found that MDM4 or USP2a also increased the mitochondrial enrichment of transcriptionally inactive p53 and promoted cell death in cisplatin-treated U251 cells. We showed that MDM4

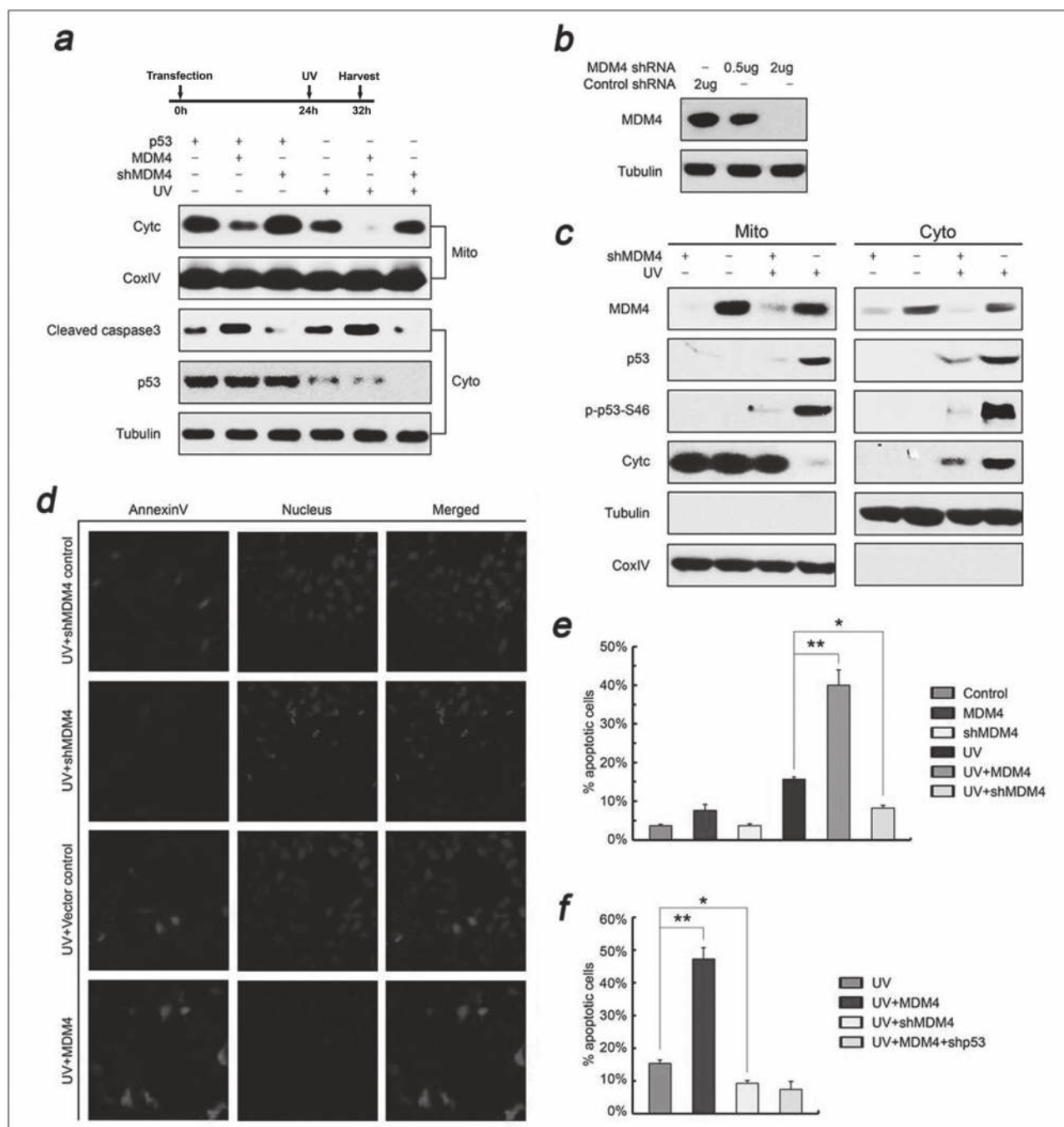


Fig. 3. MDM4 facilitates the p53-dependent mitochondrial apoptosis pathway. (a) MDM4 promoted U87MG cell apoptosis after UV irradiation or p53 overexpression. U87MG cells preinfected with lentivirus for shRNA expression as indicated were transfected with the indicated plasmids. At 24h posttransfection, the cells were irradiated with or without UV light for 8h. Then, the protein expression was determined in the whole-cell lysate and mitochondrial fraction. (b) Analysis of shRNA efficiency for MDM4 knockdown. HEK293T cells were transiently transfected with the FG12 plasmid with MDM4 shRNA or the FG12 control vector as indicated. The cell lysate was analyzed by immunoblotting with antibodies for endogenous MDM4 or tubulin. (c) Subcellular distribution of MDM4, p53, p53Ser46^P, p53S15^P and cytochrome c after UV irradiation. U87MG cells were transiently transfected with the indicated plasmids before UV irradiation, and cytoplasmic and mitochondrial fractions were analyzed by immunoblotting. Tubulin and CoxIV were used as internal controls for cytoplasmic and mitochondrial protein expression. (d) UV-induced apoptosis was inhibited by MDM4 silencing in U87MG cells. U87MG cells were infected with MDM4 shRNA lentivirus. The cells were incubated with annexin V and Hoechst nuclear staining before examination by confocal microscopy. (e) Overexpression of MDM4 enhanced apoptosis induced by UV irradiation. U87MG cell lines were treated with UV irradiation or left unirradiated after transfection with MDM4 or infection with MDM4 shRNA lentivirus and then analyzed for apoptosis by an annexin V assay. Experiments were performed at least three times, and the representative results were shown. (f) MDM4 facilitated p53-dependent apoptosis in response to UV irradiation. U87MG cell lines were treated with UV irradiation after infection with MDM4 shRNA or p53 shRNA lentivirus and then analyzed for apoptosis by the annexin V assay. Experiments were performed at least three times, and the representative results were shown.

facilitated apoptosis through a p53-, but not p21-, dependent pathway (Figures 5f and h). Thus, p53-mediated mitochondrial apoptosis, not p53 transcription-dependent apoptosis, was the dominant pathway in UV-treated U87MG cells.

MDM4 also bound to BCL2 (Figure 4d), and MDM4 seemingly did not function as a BCL2 anchor based on the fact that MDM4 depletion did not alter the presence of BCL2 in the mitochondria (11). This interaction may not result in the intrinsic apoptotic response.

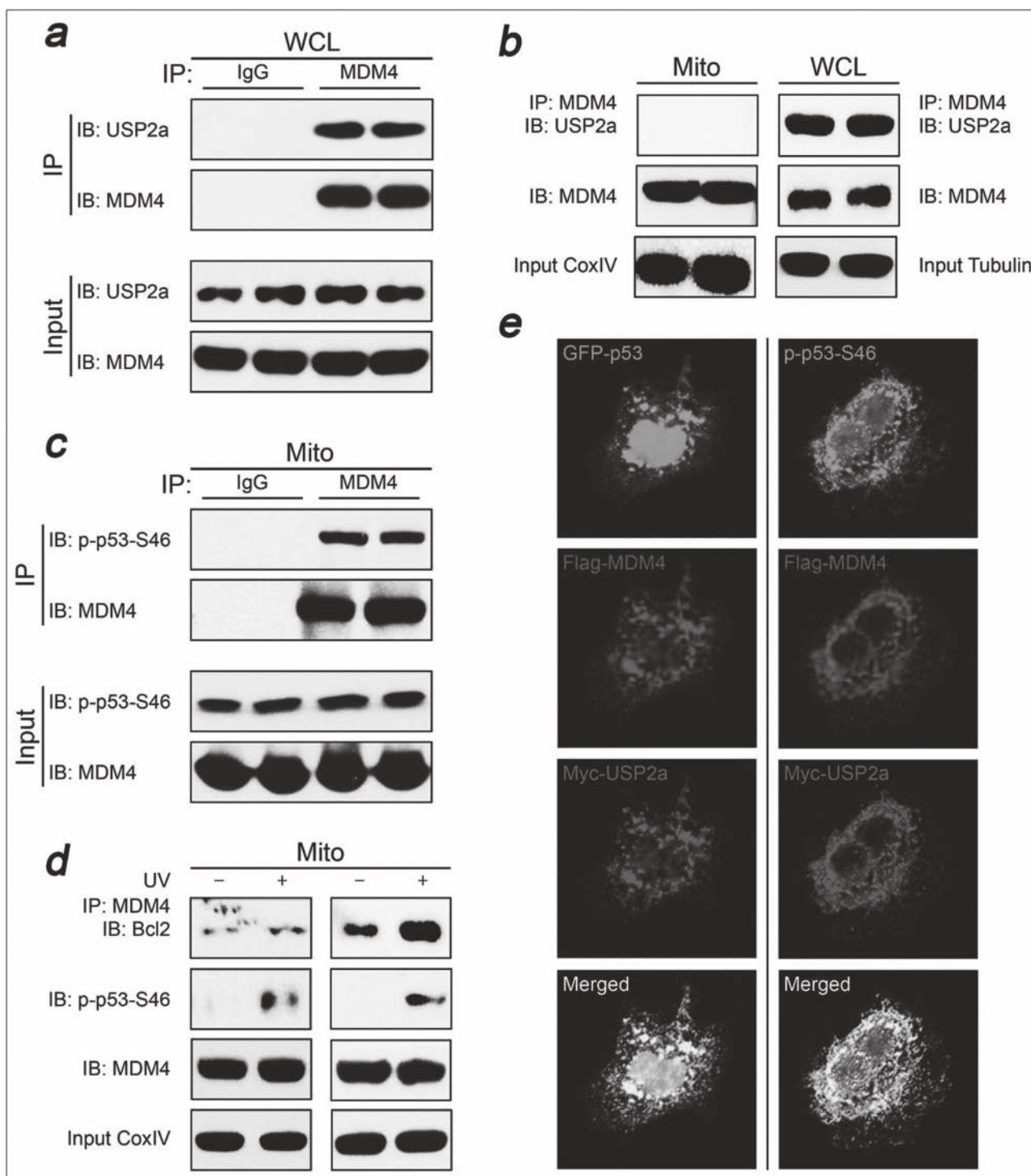


Fig. 4. Interaction of MDM4 with p53Ser46^P, USP2a and Bcl2 in U87MG cells. (a) MDM4 interacted with USP2a in U87MG cells. Whole-cell lysates were immunoprecipitated with anti-MDM4 antibody and analyzed by immunoblotting with anti-USP2a antibody and anti-MDM4 antibody. Separate aliquots of the lysates were immunoblotted with the indicated antibodies. (b) The interaction between MDM4 and USP2a was present in cytoplasmic but not mitochondrial extracts. Whole-cell lysates and mitochondrial extracts were immunoprecipitated with anti-MDM4 antibody and analyzed by immunoblotting with anti-USP2a and anti-MDM4 antibodies. (c) MDM4 interacted with p53Ser46^P in the mitochondria from U87MG cells treated with UV irradiation. Mitochondrial extracts were immunoprecipitated with anti-MDM4 antibody and analyzed by immunoblotting with anti-p53Ser46^P and anti-MDM4 antibodies. Separate aliquots of the lysates were immunoblotted with the indicated antibodies. (d) MDM4 formed a complex with p53Ser46^P and Bcl2 in mitochondria from UV-treated U87MG cells. Mitochondrial extracts were immunoprecipitated with anti-MDM4 antibody and analyzed by immunoblotting with anti-p53Ser46^P antibody, anti-Bcl2 antibody or anti-MDM4 antibody. The purity of the mitochondrial extract was determined by immunoblotting with anti-CoxIV antibody. Two repeated experiments were shown in the left and right panels. The Bcl2 in the right panel was resulted from the longer time of exposure on the film. (e) Determination of colocalization of p53, p53Ser46^P, MDM4 and USP2a by immunofluorescence. U87MG cells were transfected with GFP-p53, Flag-MDM4 and Myc-USP2a or with p53, Flag-MDM4 and Myc-USP2a. The cells were examined by confocal microscopy.

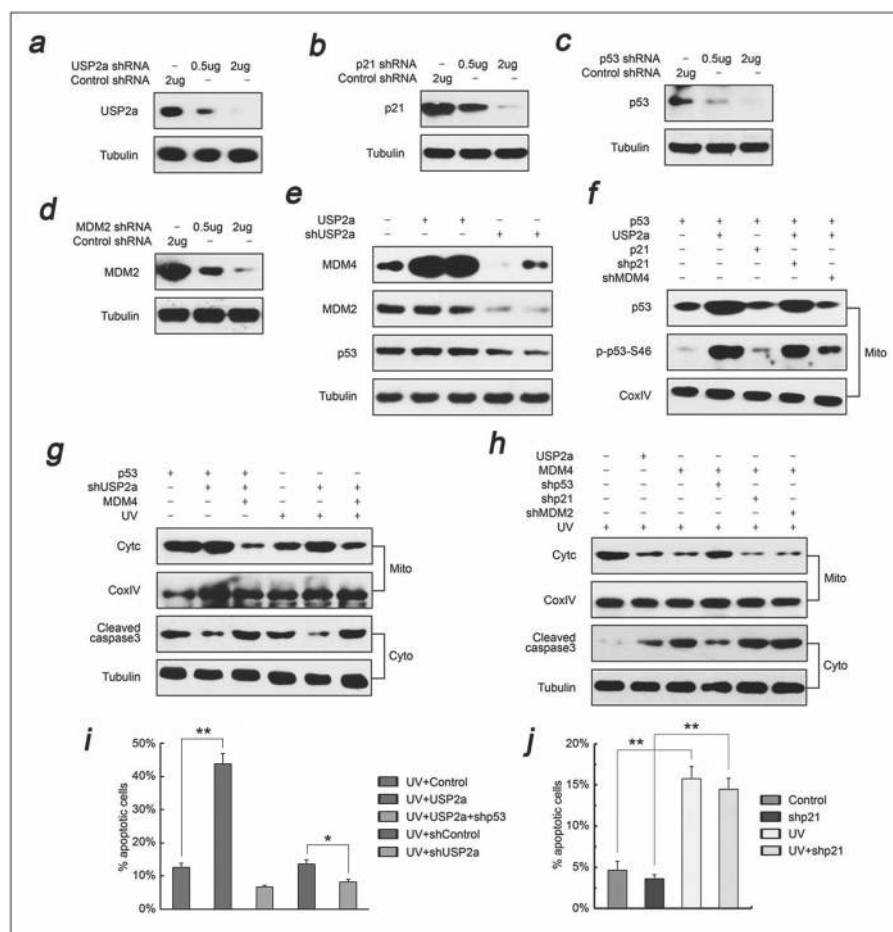


Fig. 5. MDM4 is stabilized by USP2a and promotes p53-dependent UV-evoked apoptosis. (a–d) Analysis of shRNA efficiency for USP2a, p21, p53 and MDM2 knockdown. HEK293T cells were transiently transfected with the FG12 plasmid with shRNAs or the FG12 control vector as indicated. The cell lysates were analyzed by immunoblotting with antibodies for endogenous USP2a, p21, MDM2, p53 and tubulin. (e) USP2a stabilized MDM4 protein. U87MG cells were transfected with USP2a or the shRNA for USP2a. Protein levels in whole-cell extracts were analyzed by immunoblotting. (f) USP2a increased the mitochondrial localization of p53 and p53Ser46^P in the presence of MDM4. U87MG cells were transfected with the indicated plasmids. Protein levels in the mitochondrial extract were analyzed by immunoblotting. (g) MDM4 promoted apoptosis of U87MG cells induced by UV or p53 overexpression after USP2a knockdown. After transfection with the indicated plasmids, U87MG cells were treated with UV or left unirradiated. The whole-cell extracts and mitochondrial fractions were analyzed by immunoblotting. (h) MDM4 promoted apoptosis through the p53-mediated intrinsic way independent of p21. After transfection with the indicated plasmids, U87MG cells were treated with UV irradiation. The whole-cell extracts or mitochondrial fractions were analyzed by immunoblotting. (i) USP2a overexpression enhanced p53-dependent apoptosis in response to UV irradiation. U87MG cells were treated with UV irradiation after transfection with the indicated plasmids and then were analyzed for apoptosis by annexin V assay. Experiments were performed at least three times, and the representative results were shown. (j) p21 had no effect on UV-evoked apoptosis. U87MG cells were treated with UV irradiation after transfection with the indicated plasmids and then were analyzed for apoptosis by annexin V assay. Experiments were performed at least three times, and the representative results were shown.

A reduction in endogenous MDM4 levels caused a specific decrease in mitochondrial p53, particularly of p53Ser46^P, which was accompanied by a reduction in intrinsic apoptosis (Figure 3c). The presence of MDM4 in the mitochondria led us to hypothesize that MDM4 may affect p53-mediated mitochondrial apoptosis.

Reduced MDM4 protein expression correlates with faster progression and poorer survival in several cancer types (37). In this study, our data indicated that high expression levels of MDM4 and USP2a have beneficial effects on glioblastoma prognosis and that the molecular mechanism underlying this phenomenon is through the induction of p53-dependent mitochondrial apoptosis. The positive regulation of p53 function by MDM4 challenges the current dogma of MDM4 activity. Although different models have been proposed to explain the negative regulation exerted by MDM4 toward p53, these models generally apply to regulation at basal or sublethal conditions. Indeed, the antagonistic function of MDM4 toward cell viability often concurs with highly increased levels of MDM2 and p21, both of which are events resembling a growth arrest response

(38). On the contrary, the data reported here refer to a function of MDM4 during lethal genotoxic stress, particularly in the intrinsic p53 apoptotic pathway.

Supplementary material

Supplementary Table S1 and Figures S1–S4 can be found at <http://carcin.oxfordjournals.org/>

Funding

National Natural Science Foundation of China (30930094 and 81371382); National Natural Science Foundation of China for Youth (81302188); National Sciences Fund Project of Anhui Province, China (11040606M212).

Conflict of Interest Statement: None declared.

References

1. Ohgaki,H. *et al.* (2005) Epidemiology and etiology of gliomas. *Acta Neuropathol.*, **109**, 93–108.
2. Ohgaki,H. (2009) Epidemiology of brain tumors. *Methods Mol. Biol.*, **472**, 323–342.
3. Stegh,A.H. *et al.* (2011) Beyond effector caspase inhibition: Bcl2L12 neutralizes p53 signaling in glioblastoma. *Cell Cycle*, **10**, 33–38.
4. Marine,J.C. *et al.* (2006) Keeping p53 in check: essential and synergistic functions of Mdm2 and Mdm4. *Cell Death Differ.*, **13**, 927–934.
5. Toledo,F. *et al.* (2007) MDM2 and MDM4: p53 regulators as targets in anticancer therapy. *Int. J. Biochem. Cell Biol.*, **39**, 1476–1482.
6. Steinman,H.A. *et al.* (2005) Rescue of Mdm4-deficient mice by Mdm2 reveals functional overlap of Mdm2 and Mdm4 in development. *Oncogene*, **24**, 7935–7940.
7. Barboza,J.A. *et al.* (2008) Mdm2 and Mdm4 loss regulates distinct p53 activities. *Mol. Cancer Res.*, **6**, 947–954.
8. Jackson,M.W. *et al.* (2000) MdmX protects p53 from Mdm2-mediated degradation. *Mol. Cell. Biol.*, **20**, 1001–1007.
9. Stad,R. *et al.* (2000) Hdmx stabilizes Mdm2 and p53. *J. Biol. Chem.*, **275**, 28039–28044.
10. Mancini,F. *et al.* (2004) MDM4 (MDMX) overexpression enhances stabilization of stress-induced p53 and promotes apoptosis. *J. Biol. Chem.*, **279**, 8169–8180.
11. Mancini,F. *et al.* (2009) MDM4 (MDMX) localizes at the mitochondria and facilitates the p53-mediated intrinsic-apoptotic pathway. *EMBO J.*, **28**, 1926–1939.
12. Riemenschneider,M.J. *et al.* (1999) Amplification and overexpression of the MDM4 (MDMX) gene from 1q32 in a subset of malignant gliomas without TP53 mutation or MDM2 amplification. *Cancer Res.*, **59**, 6091–6096.
13. Riemenschneider,M.J. *et al.* (2003) Refined mapping of 1q32 amplicons in malignant gliomas confirms MDM4 as the main amplification target. *Int. J. Cancer*, **104**, 752–757.
14. Kruse,J.P. *et al.* (2009) Modes of p53 regulation. *Cell*, **137**, 609–622.
15. Vogelstein,B. *et al.* (2000) Surfing the p53 network. *Nature*, **408**, 307–310.
16. Greenblatt,M.S. *et al.* (1994) Mutations in the p53 tumor suppressor gene: clues to cancer etiology and molecular pathogenesis. *Cancer Res.*, **54**, 4855–4878.
17. Chipuk,J.E. *et al.* (2006) Dissecting p53-dependent apoptosis. *Cell Death Differ.*, **13**, 994–1002.
18. Chipuk,J.E. *et al.* (2004) Direct activation of Bax by p53 mediates mitochondrial membrane permeabilization and apoptosis. *Science*, **303**, 1010–1014.
19. Marchenko,N.D. *et al.* (2000) Death signal-induced localization of p53 protein to mitochondria. A potential role in apoptotic signaling. *J. Biol. Chem.*, **275**, 16202–16212.
20. Amerik,A.Y. *et al.* (2004) Mechanism and function of deubiquitinating enzymes. *Biochim. Biophys. Acta*, **1695**, 189–207.
21. Wilkinson,K.D. (2000) Ubiquitination and deubiquitination: targeting of proteins for degradation by the proteasome. *Semin. Cell Dev. Biol.*, **11**, 141–148.
22. Stevenson,L.F. *et al.* (2007) The deubiquitinating enzyme USP2a regulates the p53 pathway by targeting Mdm2. *EMBO J.*, **26**, 976–986.
23. Priolo,C. *et al.* (2006) The isopeptidase USP2a protects human prostate cancer from apoptosis. *Cancer Res.*, **66**, 8625–8632.
24. Allende-Vega,N. *et al.* (2010) MdmX is a substrate for the deubiquitinating enzyme USP2a. *Oncogene*, **29**, 432–441.
25. Tiscornia,G. *et al.* (2006) Production and purification of lentiviral vectors. *Nat. Protoc.*, **1**, 241–245.
26. Mancini,F. *et al.* (2009) Mitochondrial MDM4 (MDMX): an unpredicted role in the p53-mediated intrinsic apoptotic pathway. *Cell Cycle*, **8**, 3854–3859.
27. Parant,J. *et al.* (2001) Rescue of embryonic lethality in Mdm4-null mice by loss of Trp53 suggests a nonoverlapping pathway with MDM2 to regulate p53. *Nat. Genet.*, **29**, 92–95.
28. Jin,G. *et al.* (2010) HDMX regulates p53 activity and confers chemoresistance to 3-bis(2-chloroethyl)-1-nitrosourea. *Neuro. Oncol.*, **12**, 956–966.
29. Nemajerova,A. *et al.* (2005) The post-translational phosphorylation and acetylation modification profile is not the determining factor in targeting endogenous stress-induced p53 to mitochondria. *Cell Death Differ.*, **12**, 197–200.
30. Feng,L. *et al.* (2006) Ser46 phosphorylation regulates p53-dependent apoptosis and replicative senescence. *Cell Cycle*, **5**, 2812–2819.
31. Moll,U.M. *et al.* (2005) Transcription-independent pro-apoptotic functions of p53. *Curr. Opin. Cell Biol.*, **17**, 631–636.
32. Böttger,V. *et al.* (1999) Comparative study of the p53-mdm2 and p53-MDMX interfaces. *Oncogene*, **18**, 189–199.
33. Shvarts,A. *et al.* (1996) MDMX: a novel p53-binding protein with some functional properties of MDM2. *EMBO J.*, **15**, 5349–5357.
34. Chen,P. *et al.* (1995) Constitutional p53 mutations associated with brain tumors in young adults. *Cancer Genet. Cytogenet.*, **82**, 106–115.
35. Frebourg,T. *et al.* (1992) A functional screen for germ line p53 mutations based on transcriptional activation. *Cancer Res.*, **52**, 6976–6978.
36. Yang,X. *et al.* (2006) Akt-mediated cisplatin resistance in ovarian cancer: modulation of p53 action on caspase-dependent mitochondrial death pathway. *Cancer Res.*, **66**, 3126–3136.
37. Lenos,K. *et al.* (2012) Alternate splicing of the p53 inhibitor HDMX offers a superior prognostic biomarker than p53 mutation in human cancer. *Cancer Res.*, **72**, 4074–4084.
38. Gilkes,D.M. *et al.* (2006) MDMX regulation of p53 response to ribosomal stress. *EMBO J.*, **25**, 5614–5625.

Received September 11, 2013; revised January 2, 2014;
accepted January 10, 2014